Identification by ESR of Pb^{+}-type centres in lead-doped $SrCl_2$

1992 J. Phys.: Condens. Matter 4 9259

(http://iopscience.iop.org/0953-8984/4/47/008)

J. Phys.: Condens. Matter 4 (1992) 9259–9268. Printed in the UK

Identification by ESR of Pb^+-type centres in lead-doped $SrCl_2$

E Goovaerts, S V Nistor† and D Schoemaker
Physics Department, University of Antwerp (UIA) B-2610 Antwerpen-Wilrijk, Belgium

Received 7 September 1992

Abstract. Several Pb^+-type centres are produced in $SrCl_2$:$PbCl_2$ crystals by x-ray irradiation at 80 K and subsequent thermal and optical treatments. From the analysis of the electron-spin-resonance (ESR) and production properties, the dominant spectrum, with trigonal symmetry around ⟨111⟩, is attributed to a Pb^+ ion located on a cation site with an anion vacancy in a nearest-neighbour position: the so-called $Pb^+(1)$ centre with the laser-active-type structure. Specific thermal treatments lead to two more Pb^+ centres with the same symmetry. The analysis of their hyperfine interaction parameters shows that in both centres the Pb^+ ion is subject to a strong odd crystal field too, but their defect structures could not be further elucidated. An additional spectrum with a small orthorhombic distorsion is observed in a more heavily doped crystal and is attributed to a lead dimer centre consisting of a $Pb^+(1)$ defect perturbed by a nearest-neighbour substitutional Pb^{2+} impurity.

1. Introduction

Since the identification of the $Tl^0(1)$ centre in alkali halides [1,2] and the discovery of its attractive laser-active properties [3,4] the interest in the study of electron-trapped centres, produced by ionizing radiation in crystals doped with ns^2-type ions, has greatly increased. A large variety of np^1-type centres with monomer and dimer structures were observed in alkali halides doped with monovalent (M^+ = Ga^+, In^+, Tl^+) or divalent (Me^{2+} = Sn^{2+}, Ge^{2+}, Pb^{2+}) ions [5]. The formation of a large variety of electron-trapped centres in such systems is mainly due to the stabilization of negative-ion vacancies at the M^0 and Me^+ primary radiation defects respectively. The search for similar defects in other ionic crystals has to date been successful for Pb^+ in $KMgF_3$ [6] (lasing, but fading under high-power excitation) and in three alkaline-earth fluorides [7] (excited-state absorption prevents laser action [8]). Recently, we were able to produce high concentrations of two $Tl^0(1)$-type centres in $SrCl_2$:TlCl [9]. In both centres, denoted by $Tl_c^0(1)$ and $Tl_i^0(1)$, the charge-compensating anion vacancy is associated with a Tl^0 atom located in a substitutional cation site, and in an interstitial site, respectively. Further investigations of their optical properties are needed to evaluate their potential for laser applications.

In this paper we report the production of several Pb^+ centres obtained by x-ray irradiation of $SrCl_2$:$PbCl_2$ crystals. As inferred from the analysis of the electron-spin-resonance (ESR) data, the dominant centre possesses the so-called laser-active-type structure consisting of a $Pb^+(6p^1)$ ion on a cation site, with a nearest-neighbour (NN)

† On leave from the Institute of Atomic Physics—IFTM, PO Box MG-6, Bucuresti - 76900, Romania.

0953-8984/92/479259+10$07.50

anion vacancy. Its optical and thermal stability, and the relatively high concentrations which can be obtained, are favourable features in view of possible application as a laser-active material. Two more Pb^+-type ESR spectra of relatively low intensity were detected after various thermal treatments. They possess axial symmetry around ⟨111⟩ too, but their production and ESR properties yield insufficient information to determine their microscopic structures. An orthorhombic spectrum, with near ⟨111⟩ axial symmetry, observed in a crystal with a higher lead concentration, has been tentatively attributed to a $Pb^+(1)$ centre disturbed by a substitutional Pb^{2+} impurity in a NN position.

2. Experimental details

Samples of approximately $3 \times 3 \times 10$ mm^3 were cleaved from single crystals grown in closed quartz ampoules by the Bridgman technique, in a reactive atmosphere [10]. As starting material either pA or Extrapure grade $SrCl_2 \cdot 6H_2O$ (Merck) were used, from which the crystallization water was removed by warming up to 250 °C for 48 hours in vacuo (10^{-2} mm Hg). Before treating in a reactive atmosphere, 0.2 to 1 mol% of ultrapure $PbCl_2$ with lead isotopes in the natural abundance, or ^{207}Pb enriched (93%) metallic lead were added. In the last case the treatment of the melt with the argon–CCl_4 mixture was continued until all the lead dissolved in $SrCl_2$. The isotope enriched samples were helpful to unravel the ^{207}Pb hyperfine (HF) structure of the observed Pb^+-type centres. The samples were x-ray irradiated (W-anode, 50 kV, 50 mA) at 80 K or room temperature (RT), with the same set-up as described earlier [2]. Before any irradiation, the samples were warmed up to 500°C for 10 minutes and quickly cooled to RT. The ESR measurements were performed in the X-band ($\nu \approx 9.27$ GHz) on a Varian E-12 spectrometer. The variable-temperature accessory allowed measurements and pulse-anneal experiments to be performed in the 8–260 K temperature range. In order to diminish the optical bleaching effects, all experiments, excepting those otherwise mentioned, were performed under red ambient light.

3. Results

3.1. Production and ESR properties

Strong ESR lines attributed to a $Pb^+(1)$ type centre were observed at $T \leqslant 80$ K after a relatively brief (15 minutes) x-ray irradiation at RT or, alternatively, at 80 K followed by a short warm-up of the sample at $T > 140$ K. The reduced linewidth of $\Delta H_0 = 5.0 \pm 0.5$ mT, —using the relation $\Delta H = (g/g_0)\Delta H_0$ in which ΔH is the measured linewidth of the ^{even}Pb spectrum and g is the effective g-value in the direction of the static field—, was virtually independent of temperature in the T = 8–60 K range, and no saturation effects were observed down to 8 K for microwave powers of up to 50 mW. In none of the ESR lines could a superhyperfine structure be observed, even at the lowest attainable temperature ($T \simeq 8$ K), for a low amplitude of the static magnetic field modulation and low microwave powers.

An angular-variation study of the ESR spectra with the magnetic field rotated in a {110} plane (figure 1(*c*)) shows that the $Pb^+(1)$ centre possesses axial symmetry around a ⟨111⟩ direction. Spectra are shown in figures 1(*a*), (*b*), (*d*) for the external static magnetic field $\boldsymbol{H}$ oriented along ⟨110⟩, ⟨111⟩ and ⟨100⟩ directions, respectively.

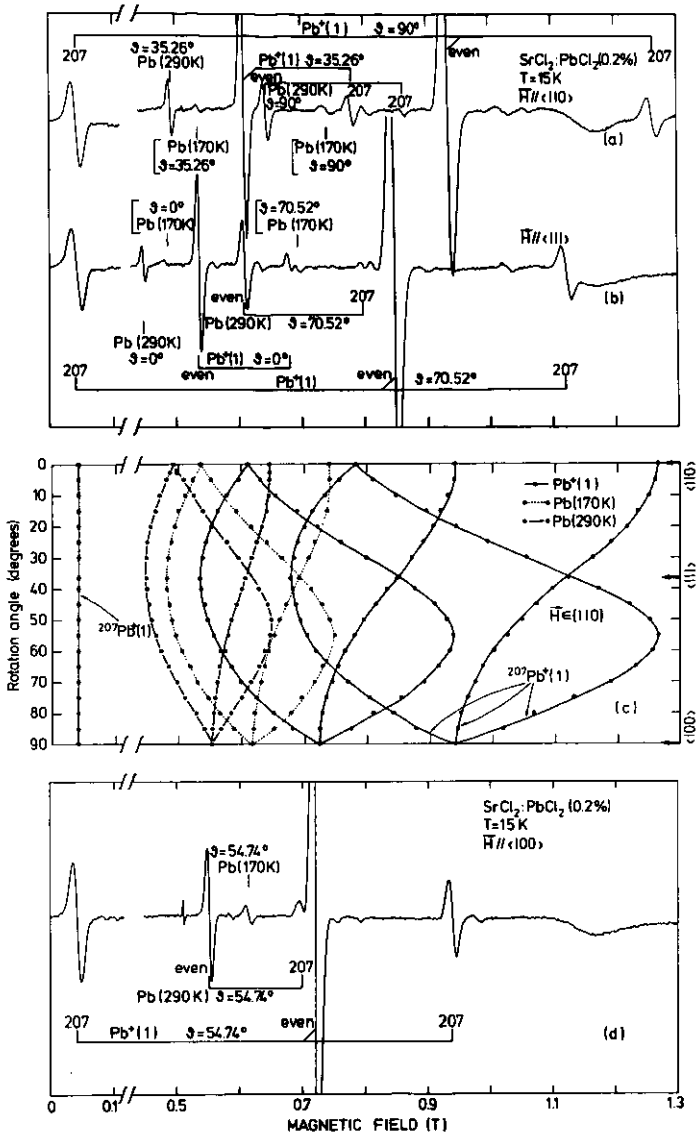

Figure 1. ESR spectra at T = 15 K of a $SrCl_2$ crystal doped with 0.2 mol% $PbCl_2$, x-ray irradiated for 30 min at 80 K and pulse annealed at 270 K with (*a*) $\boldsymbol{H}\|\{100\}$, (*b*) $\boldsymbol{H}\|\{111\}$ and (*d*) $\boldsymbol{H}\|\{100\}$. (*c*) shows the angular variation in a {110} plane of the ESR lines positions of the $Pb^+(1)$, Pb(170 K) and Pb(290 K) centres for the even ($I = 0$) isotope lines, as well as for the hyperfine components ($I = \frac{1}{2}$) of the ^{207}Pb isotope centre. The experimental data represented by dots are compared to angular variation calculated with the spin-Hamiltonian parameters from table 1.

The strong central lines belong to ESR transitions of $Pb^+(1)$ centres containing ^{even}Pb isotopes ($I = 0$, natural abundance 79%) which have no nuclear spin. The low- and high-field lines are due to ESR transitions from $Pb^+(1)$ centres containing the 21% abundant ^{207}Pb isotope with nuclear spin $I = \frac{1}{2}$. The ESR spectrum exhibits a pure

axial ⟨111⟩ character in the whole temperature range of the measurements (8–60 K), without tipping or lower symmetry-distortion effects.

Pulse annealing experiments show (figure 2) that the small concentration of $Pb^+(1)$ centres produced after x-ray irradiation at $T=80$ K, increases by at least an order of magnitude by warming up the sample to 180 K. As shown earlier by optical spectroscopy of low-temperature irradiated $SrCl_2$ crystals [11], bands attributed to M-type centres grow above 130 K, reaching maximum intensity at 180 K. This process can be associated with the onset of the motion of anion vacancies in the $SrCl_2$ lattice.

The concentration of $Pb^+(1)$ centres decreases above $T=210$ K, probably by recombination with the V_K-type centres which decay in this temperature range (figure 2). The concentration of $Pb^+(1)$ centres can be restored by further x-ray irradiation at RT. A slight increase (~10%) in the concentration of the $Pb^+(1)$ centres produced by irradiation at RT in the dark could be obtained by subsequent white-light bleaching for a few minutes.

It is worthwhile mentioning that the resulting concentrations of various Pb^+-type defects, after annealing above 250 K, depend to some extent on the thermal history of the sample before irradiation and its impurity content.

In a crystal doped with a high nominal Pb concentration in the melt (1 mol%) a spectrum has been detected, which we tentatively attribute to a lead dimer defect, which it is proposed to call $Pb^+(1)Pb^{2+}$ (see section 4). It possesses an angular variation of the ESR transitions very similar to that of the $Pb^+(1)$ centre, but with a small splitting of the lines in the field direction perpendicular to the main defect axis (90° lines for the magnetic field along ⟨110⟩), due to a small orthorhombic distortion (figure 3). In fact, for several orientations the transitions are obscured by the intense neighbouring $Pb^+(1)$ lines. The production properties of this centre (figure 2) are quite similar to those of the main Pb^+ centre, with two differences. Firstly, no ESR lines attributed to the $Pb^+(1)Pb^{2+}$ centre were observed after the low-temperature irradiation, which might be due to their relatively low concentration. Secondly, their concentration does not decrease as much by pulse annealing above 210 K.

Additional ESR transitions with lower intensity than those of the main $Pb^+(1)$ centre have been observed by pulse annealing the samples x-ray irradiated at 80 K (see figure 2). From the analysis of the ESR spectra it has been found that they belong to two Pb^+-type centres.

In the 150–170 K temperature range the Pb^+-type defect, denoted by $Pb^+(170)$, is created. It reaches its maximum concentration at $T=170$ K, and starts decaying at higher temperatures (figure 2). However, a sizable amount of such centres can still be produced by irradiation at 80 K followed by a short annealing at 290 K. The $Pb^+(170\text{ K})$ centre exhibits pure ⟨111⟩ trigonal symmetry as inferred from the angular dependence of the ESR lines (figure 1(*c*)).

Another paramagnetic centre with the same symmetry, named $Pb^+(290\text{ K})$, is produced by irradiation at 80 K and subsequent thermal anneal above 250 K (figure 2), or directly by irradiation at RT. The centre is bleached at RT by ambient white light. Optimal production was obtained by a very short pulse annealing at RT (≈2 min) in red ambient light.

3.2. Analysis of the ESR spectra

The ESR spectra of the Pb^+-type defects observed in the x-ray-irradiated $SrCl_2$:$PbCl_2$ crystals are described by the spin Hamiltonian

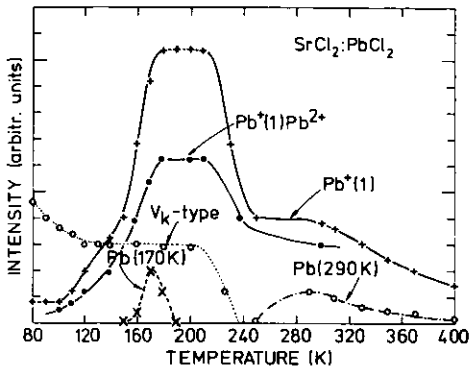

Figure 2. The thermal growth and decay (under ambient red light) of the paramagnetic lead associated centres in a $SrCl_2$:$PbCl_2$ crystal x-ray irradiated for 30 min at T = 80 K. The intensity of the ESR lines was measured at T = 60 K, for $H \| \langle 111 \rangle$ after consecutive anneals of 3 minutes to temperatures above 80 K. The relative variation in the intensity of ESR lines attributed to V_K-type centres is also presented. After the pulse anneal at 250 K the pulse annealings were subsequently carried out from T = 290 K. The relative intensities of various centres are arbitrary.

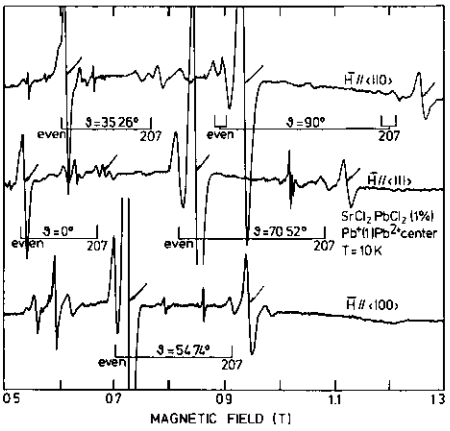

Figure 3. ESR spectra at T = 10 K of a $SrCl_2$ crystal doped with 1 mol% $PbCl_2$, x-ray irradiated for 30 min at 80 K and pulse annealed at 290 K, with the magnetic field oriented along the main crystal axes. The lines attributed to the $Pb^+(1)Pb^{2+}$ centre are indicated by the angle between the local axial component and the magnetic field, and by the corresponding nuclear isotopes. The lines of the main $Pb^+(1)$ centre are marked by oblique arrows. The narrow lines belong to an unidentified paramagnetic impurity.

$$\mathcal{H}/g_0\mu_B = (1/g_0)\boldsymbol{H}\cdot\mathbf{g}\cdot\boldsymbol{S} + \boldsymbol{S}\cdot\mathbf{A}\cdot\boldsymbol{I} \qquad (1)$$

where $S = \frac{1}{2}$ and $I = \frac{1}{2}$. The centres containing ^{even}Pb nuclei (I=0.79% natural abundance) are described by the first term, giving rise to singlet resonance lines, which are visible in Figures 1(*a*), (*b*), (*d*) as the most intense lines in the 0.5–0.7 T range. From these lines the g-values can be determined straightforwardly, $g_i = (h\nu)/(\mu_B H_i)$, where the static field is along a principal axis of the g-tensor, H_i is the field position of the transition, h is Planck's constant and ν the microwave frequency. The **g** and **A** parameters of the defects were more accurately obtained from a fitting procedure based on a numerical diagonalization of spin Hamiltonian (1). The parameters resulting from the best least-squares fit of all the field positions for $H \| \langle 110 \rangle$, $\langle 111 \rangle$ and $\langle 100 \rangle$ of the $I = 0$ and $I = \frac{1}{2}$ ESR spectra are presented in tables 1 and 2.

They all possess the general characteristics of np^1 defects, with negative g-shifts, more pronounced for the perpendicular than for the parallel component. The g-values, HF parameters and linewidths are very similar to those of the Pb^+ centres in the alkali halides. The g-shifts are decreasing along the sequence $Pb^+(1)$, $Pb^+(1)Pb^{2+}$, Pb^+(170 K), and Pb^+(290 K), pointing to correspondingly decreasing strength of the axial crystal field. Quantitative information concerning the crystal field acting on Pb^+-type centres can be obtained from an analysis of the HF parameters in a simple crystal-field model [12, 13], in which spin–orbit coupling and an axial crystal field are considered. The HF components can be expressed in terms of the g-shifts, $\Delta g_i = g_0 - g_i$, and of the isotropic and anisotropic contributions, A_σ and ρ, of the

Table 1. Spin-Hamiltonian parameters of the Pb^+-type centres in $SrCl_2$ at T=15 K. The HF parameters $A_\perp$, $A_\parallel$, ρ and A_σ and the linewidth ΔH are given in mT. The estimated precision is 0.0004 for g-values and 0.7 mT for A-values, except for the $Pb^+(1)Pb^{2+}$ centre (table 2). The corresponding parameters for the Pb^+-type centres in other ionic crystals are given for comparison. Signs are attributed to the HF constants according to the constraint of a positive and relatively constant ρ-value through the series of Pb^+ defects (see [12, 13].)

	$g_\perp$	$g_\parallel$	$A_\perp$	$A_\parallel$	ρ	A_σ	Δ
$Pb^+(1)$ in $SrCl_2$	0.7007	1.2189	−327.0	+289.1	+79	− 88	5.
$Pb^+(1)Pb^{2+}$ in $SrCl_2$	0.730 [a]	1.240	−314 [a]	+277	+83	− 86	4.
Pb(170K) in $SrCl_2$	0.8836	1.3554	−324.2	+251.6	+80	−103	5.
Pb(290K) in $SrCl_2$	1.0165	1.4613	−293.7	+233.2	+78	− 82	4.
$Pb^+(Cl_i^-)$ in KCl [b]	1.331	1.632	−256.8	+163.5	+75	− 96	6
$Pb^+(Cl_i^-)$ in RbCl [b]	1.276	1.609	−263.5	+167.1	+74	− 97	7
Pb^+(1b) in KCl [c]	1.051	1.515	−259.5	+245	+79	− 43	
Pb^+(1b) in RbCl [c]	1.036	1.493	−272.0	+222.5	+73	− 63	
$Pb^+(1)$ in CaF_2 [d]	1.190	1.706	−166.3	+245.5	+65	+31	
$Pb^+(1)$ in SrF_2 [d]	1.167	1.711	−193.2	+222.7	+64	+4	
$Pb^+(1)$ in BaF_2 [d]	1.036	1.634	−240.5	+218.8	+66	− 26	

[a] Axial approximation. See table 2 for the full set of parameters.
[b] Data at T = 10 K from [16].
[c] Data at T = 15 K from [17].
[d] Data from [7].

Table 2. Spin-Hamiltonian parameters of the orthorhombic $Pb^+(1)Pb^{2+}$ centre in $SrCl_2$ at T= 15 K. The HF parameters are given in mT. The estimated precision is 0.001 for the g-values, and 1 mT for the A-values. The ESR parameters for a similar defect in SrF_2 are also given.

Host	g_x	g_y	g_z	A_x	A_y	A_z
$SrCl_2$[a]	0.720	0.740	1.240	−311	−317	+277
SrF_2[b]	1.370	1.422	1.715	−116.6	−116.6	+169.3

[a] Symmetry axes : $x \parallel [112]$, $y \parallel [110]$ and $z \parallel [111]$.
[b] Data from [7]. The orientation of the x and y axes relative to the crystal axes has not been specified.

HF interaction,

$$A_\perp = (1 - \tfrac{1}{2}\Delta g_\parallel)A_\sigma - (1 + \tfrac{13}{4}\Delta g_\perp - \tfrac{9}{4}\Delta g_\parallel)\rho \tag{2}$$

$$A_\parallel = (1 - \tfrac{1}{2}\Delta g_\parallel)A_\sigma + (2 + \tfrac{3}{2}\Delta g_\perp + \tfrac{1}{2}\Delta g_\parallel)\rho. \tag{3}$$

The resulting numerical values of ρ and A_σ for the Pb^+ centres in $SrCl_2$ are given in table 1, together with the corresponding values of the $Pb^+(1)$ centres in other crystal hosts. The values of the anisotropic HF contribution ρ in the Pb^+-type centres in $SrCl_2$ are consistent with those previously reported for the $Pb^+(1)$ centres in alkali chlorides and alkaline-earth fluorides.

4. Structure of the centres

The isotropic HF contribution A_σ changes, under the influence of an odd crystal field, from a negative value resulting from the exchange polarization, to a positive

value introduced by the s mixing into the ground np orbital [13]. The magnitude of the s mixing depends on the intensity of the odd crystal field and is expected to increase with the decreasing Pb^+ anion–vacancy distance. The change of A_σ from a negative value to a positive one, for the $Pb^+(1)$ centres in the lattices with fluorite structure (table 1), is consistent with the decrease in the nearest cation (anion vacancy) distance, d, along the series: $SrCl_2$ ($d = 0.302$ nm), BaF_2 ($d = 0.268$ nm), SrF_2 ($d = 0.250$ nm) and CaF_2 ($d = 0.236$ nm) and with the decrease of the g-shifts. The comparison with the alkali halides is not as straightforward due to the presence of an additional perturbing cation vacancy, but comparable isotropic HF interaction parameters are found for the $Pb^+(1)$-type centres in KCl ($d = 0.315$ nm) and RbCl ($d = 0.327$ nm), in which the anion–cation distances are only slightly larger than in $SrCl_2$.

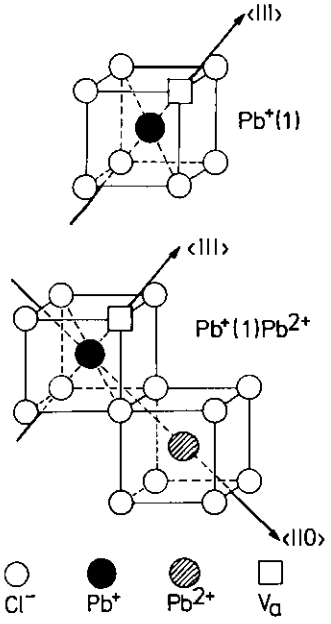

Figure 4. Structural models of the dominant $Pb^+(1)$ centre and of the dimer-type $Pb^+(1)Pb^{2+}$ centre in $SrCl_2$, as inferred from the ESR data.

The above analysis strongly suggests that the $Pb^+(1)$ centre in $SrCl_2$ consists indeed of a substitutional Pb^+ ion in a cation Sr^{2+} site, with an anion vacancy, v_a, in the NN site, along a ⟨111⟩ direction (figure 4). From the pulse annealing experiments (section 3.1) one concludes that the formation of the $Pb^+(1)$ centre in $SrCl_2$ can take place according to the reactions:

$$Pb^{2+} + e^- \rightarrow Pb^+(0) \tag{4}$$

$$Pb^+(0) + v_a \rightarrow Pb^+(1) \tag{5}$$

in which $Pb^+(0)$ stands for the primary electron-trapped lead centre without neighbouring anion vacancy. Because no charge-compensating anion vacancies are initially available in the crystal, unlike the case of Tl^+-doped $SrCl_2$ crystals [9], only a small amount of $Pb^+(1)$ centres are produced by direct irradiation at 80 K. Probably this is made possible by the stabilization of anion vacancies created in the close

vicinity of the Pb^+ ions. A larger amount of vacancies are produced as F centres in the crystals, by low-temperature irradiation. They become mobile at $T > 130$ K in $SrCl_2$, as shown from the study of F-centre aggregation [11], and the resulting vacancies are then trapped at the primary $Pb^+(0)$ centres. The trapping of the anion vacancy (reaction (5)) is favoured by the charge-compensation mechanism.

The $Pb^+(1)Pb^{2+}$ centre possesses ESR parameters very close to those of the $Pb^+(1)$ defect and is produced at temperatures where the anion vacancies are mobile, in crystals with a higher Pb^{2+} doping. It possesses orthorhombic, but near-trigonal, symmetry with principal axes along , e.g., $[11\bar{2}]$, $[1\bar{1}0]$ and [111]. The suggested structure for this defect is a $Pb^+(1)$ centre weakly disturbed by a substitutional Pb^{2+} impurity on an NN cation site (figure 4). Such a defect has also been reported in SrF_2:PbF_2 crystals, and the changes in ESR parameters from $Pb^+(1)$ to $Pb^+(1)Pb^{2+}$ are very similar in SrF_2 and $SrCl_2$ (see table 2).

It is not straightforward to propose definite models for the other two paramagnetic centres observed in irradiated $SrCl_2$:$PbCl_2$ crystals. Two simple defect models possessing trigonal symmetry can be envisaged:

(i) The $Pb^+(1)$ centre can trap a second vacancy at a site opposite to the previous one, which we call the $Pb^+(2)$ structure. This is analogous to the $Tl^0(2)$ centre in KCl [2], and could be the precursor for a $Pb^0(2)$ centre which was previously studied in SrF_2 [7, 14]. The formation of the $Pb^+(170\ K)$ centre in the temperature range where a large amount of mobile anion vacancies are available (i.e. where the formation rate of $Pb^+(1)$ centres is maximum), would make it the most suitable candidate. However, in this symmetrical configuration of vacancies the crystal field on the Pb^+ ion would contain only an even contribution, no s mixing would occur, and a significantly larger negative contribution to the isotropic HF interaction A_σ would be expected. For $Pb^+(170\ K)$ this is hardly the case (see table 1). This difficulty can, however, be circumvented by accepting that the Pb^+ ion is displaced from its normal lattice site towards one of the vacancies, in a ⟨111⟩ direction, due to the large cage dimensions in $SrCl_2$. In this case the trigonal symmetry and the presence of an odd crystal field component would be accounted for.

(ii) An alternative model agreeing with both conditions consists of a $Pb^+(1)$ centre in which the Pb^+ ion has jumped from its substitutional site, through the vacancy towards the interstitial site in a ⟨111⟩ direction from the vacancy. In thallium-doped crystals we have observed the analogous transformation of the primary $Tl_c^0(1)$ centre into the interstitial $Tl_i^0(1)$ centre. However, one would expect this process to proceed until all of the $Pb^+(1)$ centres have been transformed, which is in contradiction with the experimental results (figure 2). This transformation is expected to be complete at higher temperatures, in contradiction to our observation for the Pb^+ centres.

For both $Pb^+(170\ K)$ and $Pb^+(290\ K)$ defects, with low concentrations compared to the main $Pb^+(1)$, unintentional impurities originating in the starting materials could be part of their microscopic structures. Such impurities are expected to occur in our $SrCl_2$ crystals at higher levels than in well prepared alkali halide crystals. Indeed, semi-quantitative spectrographic analysis, performed on samples from the as-grown crystals, point to the presence of the following trace elements in concentrations less than 5 ppm: Si, Mg, Cu, Ag, Ca and Na.

It should be mentioned that, as in the case of the alkali halides, the primary $Pb^+(0)$ centre, for which a large concentration is expected to be produced directly by x-ray irradiation at low temperatures, cannot be observed in ESR although it should

be paramagnetic. Also, it was not possible to detect $Pb^{3+}(6s)$-type ESR spectra, which would result from hole trapping at the Pb^{2+} impurities, as was observed in the alkali halides [15].

5. Conclusions

After x-ray irradiation at low temperatures and subsequent warm-up, or upon direct irradiation above $T = 160$ K, $SrCl_2$:$PbCl_2$ crystals exhibit strong ESR spectra attributed to $Pb^+(1)$ centres. These defects possess the laser-active type structure, consisting of a substitutional $Pb^+(6p^1)$ ion with a NN anion vacancy. The structural model is supported by the analysis of the ESR data with the model developed earlier for an np^1 atom in an axial crystal field, and further by the production and thermal annealing properties. This demonstrates the possibility of producing such Pb^+ centres in $SrCl_2$ without perturbation by cation vacancies, which in alkali halides are unavoidably present for charge compensation in the neighbourhood of the Pb^+ ion. The ESR spectra of three more Pb^+ defects, with relatively low concentration, were also identified. One of them, which was observed in a heavily lead-doped crystal and which exhibits a small orthorhombic distortion, has been attributed to a $Pb^+(1)Pb^{2+}$ dimer centre. In spite of a careful search, neither the primary electron-trapped nor the primary hole-trapped defects, $6p^1$ $Pb^+(0)$ and $6s^1$ Pb^{3+} respectively, could be observed in any of the x-ray-irradiated $SrCl_2$:$PbCl_2$ crystals.

The $Pb^+(1)$ centre in $SrCl_2$ is stable at room temperature and exhibits good optical stability. Moreover, it can be produced in much higher concentration, than is the case with alkali halide hosts. These properties make the $SrCl_2$:$Pb^+(1)$ system an attractive candidate as a laser-active material.

Acknowledgments

The authors are indebted to A Bouwen for expert assistance and to C D Mateescu and Ch Ciucur for help in growing and characterizing the crystals employed in this study. Financial support from the Belgian National Fund for Scientific Research (NFWO) for one of the authors (EG) and from the Belgian Ministry of Science Policy (DPWB) for another author (SVN) is gratefully acknowledged. This work was made possible through the financial support from the Interuniversity Institute for Nuclear Sciences (IIKW), Belgium and the Ministry of Education and Science of Romania.

References

[1] Schoemaker D, Goovaerts E and Nistor S V 1978 *Bull. Am. Phys. Soc.* **23** 200
[2] Goovaerts E, Andriessen J, Nistor S V and Schoemaker D 1981 *Phys. Rev.* B **24** 29
[3] Gellerman W, Luty F and Pollock C R 1981 *Opt. Commun.* **39** 391
[4] Mollenauer L F, Vieira N D and Szeto L 1982 *Opt. Lett.* **7** 414
[5] Nistor S V, Ursu I, Goovaerts E and Schoemaker D 1986 *Rev. Roum. Phys.* **31** 865 and references therein
[6] Hörsch G and Paus H J 1987 *Opt. Commun.* **60** 69
[7] Fockele M, Lohse L, Spaeth J M and Bartram R H 1989 *J. Phys.: Condens. Matter* **1** 13
[8] Spaeth J M, Bartram R H, Rac M and Fockele M 1991 *J. Phys.: Condens. Matter* **3** 5013
[9] Nistor S V, Goovaerts E and Schoemaker D 1990 *Phys. Rev.* B **42** 7747

[10] Nistor S V 1988 *Solid State Commun.* **66** 995
[11] Matei L 1971 *Solid State Commun.* **9** 1281
[12] Heyndericlcx I, Goovaerts E and Schoemaker D 1985 *Solid State Commun.* **55** 877
[13] Schoemaker D, Heyndericlcx I and Goovaerts E 1985 *Phys. Rev.* B **31** 5687
[14] Bartram R H, Fockele M, Lohse F and Spaeth J M 1989 *J. Phys.: Condens. Matter* **1** 27
[15] Dreybrodt W and Silber D 1967 *Phys. Status Solidi* **20** 337
[16] Goovaerts E, Nistor S V and Schoemaker D 1983 *Phys. Rev.* B **28** 3712
[17] Heyndericlcx I, Goovaerts E, Nistor S V and Schoemaker D 1986 *Phys. Status Solidi* b **136** 69